Analysis of the Transmission Mechanism of NMR Spin−Spin Coupling Constants Using Fermi Contact Spin Density Distribution, Partial Spin Polarization, and Orbital Currents: XH_n Molecules

Anan Wu, Jürgen Gräfenstein, and Dieter Cremer*

Department of Theoretical Chemistry, Göteborg University Reutersgatan 2, S-41320 Göteborg, Sweden

Received: April 29, 2003; In Final Form: June 17, 2003

Trends in calculated and measured one-bond reduced spin−spin coupling constants (SSCCs) ^1K(XH) for twelve XH_n hydrides (X = C, Si, Ge, N, P, As, O, S, Se, F, Cl, Br) are explained using orbital contributions obtained with the J-**OC**-PSP (decomposition of *J* into *O*rbital *C*ontributions using the *O*rbital *C*urrents and *P*artial *S*pin *P*olarization) approach. The sign and magnitudes of the orbital contributions can be rationalized with the help of the Fermi contact spin density distribution, the s-density of an orbital at the nucleus, the electronegativity, and the polarizability of the central atom X. Partitioning of Fermi contact, the paramagnetic spin−orbit, the diamagnetic spin−orbit, and the spin dipole terms as well as the total SSCC ^nK into one-orbital contributions $^nK^k$ and orbital interaction contributions $^nK^{k,l}$ (*n*, type of SSCC; *k* and *l*, indices of occupied orbitals) reveals that each of the four Ramsey terms adds to the spin−spin coupling mechanism; however, many of the orbital contributions cancel each other so that, for example, DSO and SD terms make only negligible contributions to ^1K(XH). The two types of orbital contributions are associated with two different transmission mechanisms via the exchange antisymmetry property of the wave function. $^nK^k$ is the result of an orbital relaxation mechanism whereas $^nK^{k,l}$ is closely related to the concept of steric exchange antisymmetry. Trends in measured ^1K(XH) SSCCs can be explained by an interplay of bond and lone pair contributions. Sign and magnitude of ^1K(XH) are rationalized by utilizing the nodal behavior of zeroth- and first-order orbitals. Results are converted into simple Dirac models.

1. Introduction

Indirect scalar NMR spin−spin coupling constants (SSCCs) are sensitive antennas, which help to describe the electronic structure, geometry, and conformation of a molecule.[1−8] One-bond coupling constants ^1J reflect the nature of the chemical bond; geminal coupling constants ^2J depend on the bond angle, and by this they are sensitive to bond angle strain. Also, vicinal SSCC ^3J change in a characteristic way with the dihedral angle of a three-bond fragment, which is exploited in the Karplus relationships.[9−11] In the last 50 years an enormous amount of experimental SSCCs has been collected and used to describe electronic, geometric, and conformational features of molecules.[1−11] Various attempts have been made to relate the SSCCs of a molecule to its wave function and the orbitals constituting the wave function[1,12−16] where especially the work carried out by Contreras and co-workers[4,5,13−15] has to be mentioned. Most of this work focused on the Fermi contact (FC) contribution to the isotropic scalar SSCC and/or was carried out with semiempirical quantum chemical methods[4,5,13,14] whereas more recent work was also done at the ab initio level of theory.[15]

So far, however, no systematic approach has been presented to decompose the four Ramsey terms[17] of the indirect scalar SSCCs of a molecule, namely FC, paramagnetic spin−orbit (PSO), diamagnetic spin−orbit (DSO), and spin dipole (SD) term, into orbital contributions based on first principles. We have recently developed a couple-perturbed DFT (CPDFT) method for calculating NMR SSCCs,[18] which leads to surprisingly accurate values for most nuclei combinations.[11,19] On the basis of the CPDFT method, we have also developed the decomposition of *J* into *O*rbital *C*ontributions using *O*rbital *C*urrents and *P*artial *S*pin *P*olarization (J-OC−OC−PSP = J-**OC**-PSP).[20] The investigation of orbital currents is relevant for the understanding of DSO and PSO terms whereas spin polarization is associated with FC and SD terms. J-**OC**-PSP partitions ^nJ into one-orbital contributions $^nJ^k$ and orbital interaction contributions $^nJ^{k,l}$ (*n*, type of SSCC; *k* and *l*, orbital indices). The two types of orbital contributions are associated with two different coupling transmission mechanisms via the exchange antisymmetry property of the wave function: $^nJ^k$ is the result of an orbital relaxation mechanism whereas $^nJ^{k,l}$ is closely related to the concept of steric exchange antisymmetry.[20]

The J-**OC**-PSP approach can be carried out for any type of orbital; however, first tests have shown that the use of Boys localized molecular orbitals (LMOs) facilitates the interpretation of the calculated orbital contributions. The sum of orbital contributions is identical to the total SSCC or one of its Ramsey terms; i.e., each orbital contribution can be directly connected to the physical basis of the coupling transmission process.

In this work, we will demonstrate the usefulness of J-**OC**-PSP by analyzing the one-bond coupling constant of twelve XH_n hydrides (X = C, Si, Ge, N, P, As, O, S, Se, F, Cl, Br) in dependence of the atomic number *Z* of atom X. Experimental studies[21] have led to opposing trends for the one-bond SSCCs of group IV hydrides on one hand and those of group V, VI, or VII hydrides on the other hand. Also, it is not clear why certain hydrides of the second period do not follow the general trends within a group. The SSCC of the hydrides of the first period in the periodic table do not follow the same trend as those of the hydrides of the second and third periods. And, finally, the sign of the one-bond SSCC of the higher XH molecules could not be determined experimentally so far.

Using J-**OC**-PSP we will demonstrate that irregularities in the trends of the measured SSCC can be explained as a simple result of electronegativity and polarizability of the central atom

* Corresponding author.

10.1021/jp030541l CCC: $25.00
Published on Web 08/14/2003

X. Furthermore, we will introduce the calculation and the pictorial representation of the first-order orbitals and the Fermi contact spin density distribution as new analytic tools, which make it possible to reliably determine the sign of all FC orbital contributions so that in turn the sign of the FC term can be predicted. In a similar way, the signs of the other Ramsey contributions can be determined and by this also that of the total SSCC. One might expect that for a one-bond SSCC the bond orbital contributions are most important. However, in this work we will show that lone pair contributions are similarly important and that they actually determine the magnitude of a SSCC.

In section 2 the theory of J-**OC**-PSP is briefly summarized and the computational details of this work are described. Results of the SSCC analysis of the twelve XH_n hydrides will be presented and analyzed in section 3. In section 4, the usefulness and applicability of J-**OC**-PSP will be reviewed on the basis of the results described in this work.

2. Computational Details

The focus of the present work is on electronic processes responsible for the spin−spin coupling mechanism. Therefore, we discuss the reduced SSCC K rather than the full SSCC J to avoid a dependence on the gyromagnetic ratios of the nuclei involved.

In CPDFT, the four terms of the reduced indirect SSCC K_{AB} are given by eqs 1−4[18]

$$K_{AB}^{DSO} = \frac{2}{3}\sum_{k}^{occ}\langle\phi_k^{(0)}|\mathrm{Tr}\,\underline{\underline{h}}_{AB}^{DSO}|\phi_k^{(0)}\rangle \tag{1}$$

$$K_{AB}^{PSO} = -\frac{4}{3}\sum_{k}^{occ}\langle\phi_k^{(0)}|\mathbf{h}_A^{PSO}|\vec{\phi}_k^{(B),PSO}\rangle \tag{2}$$

$$K_{AB}^{FC} = \frac{2}{3}\sum_{k\sigma}^{occ}\langle\psi_{k\sigma}^{(0)}|\mathbf{h}_A^{FC}|\vec{\psi}_{k\sigma}^{(B),FC}\rangle \tag{3}$$

$$K_{AB}^{SD} = \frac{2}{3}\sum_{k\sigma}^{occ}\langle\psi_{k\sigma}^{(0)}|\mathbf{h}_A^{SD}|\vec{\psi}_{k\sigma}^{(B),SD}\rangle \tag{4}$$

where the DSO, PSO, FC, and SD operator are defined by eqs 5−8:

$$\underline{\underline{h}}_{AB}^{DSO} = \left\{\frac{1}{m}\left(\frac{4\pi\epsilon_0\hbar^2}{e}\right)^2\right\}\alpha^4\left(\frac{\mathbf{r}_A}{r_A^3}\cdot\frac{\mathbf{r}_B}{r_B^3}\underline{\underline{I}} - \frac{\mathbf{r}_A}{r_A^3}\circ\frac{\mathbf{r}_B}{r_B^3}\right) \tag{5}$$

$$\mathrm{h}_A^{PSO} = \left\{\frac{4\pi\epsilon_0\hbar^3}{em}\right\}\alpha^2\frac{\mathbf{r}_A}{r_A^3}\times\nabla \tag{6}$$

$$\mathbf{h}_A^{FC} = \left\{\frac{4\pi\epsilon_0\hbar^3}{em}\right\}\frac{8\pi}{3}\alpha^2\,\delta(\mathbf{r}_A)\mathbf{s} \tag{7}$$

$$\mathbf{h}_A^{SD} = \left\{\frac{4\pi\epsilon_0\hbar^3}{em}\right\}\alpha^2\left[3\frac{(\mathbf{s}\cdot\mathbf{r}_A)\mathbf{r}_A}{r_A^5} - \frac{\mathbf{s}}{r_A^3}\right] \tag{8}$$

The position of nucleus N is given by vector $\mathbf{R}_N$, $\mathbf{r}_N = \mathbf{r} - \mathbf{R}_N$, ϵ_0 is the dielectric constant of the vacuum, α is Sommerfeld's fine structure constant, $\underline{\underline{I}}$ is the unit tensor, and $\mathbf{s}$ is the electron spin in units of $\hbar$. The prefactors enclosed in braces in eqs 5−8 become equal to one in atomic units. Note that $\mathbf{h}_A^{FC}$ and $\mathbf{h}_A^{SD}$ are 2×2 matrixes with respect to the electron spin variables. The DSO and the PSO terms can be expressed in terms of spin-free orbitals ϕ_k, and the FC and SD terms are given in terms of spin-dependent orbitals ψ_k. Zeroth-order orbitals are denoted by superscript (0) whereas superscript (B) denotes first-order orbitals resulting from the perturbation at nucleus B. The indices of the occupied orbitals will be k, l, ..., those of the virtual orbitals a, b, ... The vectors $\vec{\psi}_k^{(B),X}$ and $\vec{\phi}_k^{(B),X}$ summarize the three first-order orbitals corresponding to the three components of $\mathbf{h}^{(B),X}$ (X = PSO, FC, SD).

It is straightforward to decompose the reduced SSCC K_{AB}^{DSO} into a sum of zeroth-order orbital contributions according to eq 1. For the PSO, FC, and SD terms, an orbital decomposition can be done starting from the equation for the first-order orbitals $|\vec{\psi}_{k\sigma}^{(B),X}\rangle$:

$$|\vec{\psi}_{k\sigma}^{(B),X}\rangle = \sum_{a\sigma'}^{virt}\frac{\langle\psi_{a\sigma'}^{(0)}|\mathbf{F}_B^X|\psi_{k\sigma}^{(0)}\rangle}{\epsilon_k - \epsilon_a}|\psi_{a\sigma'}^{(0)}\rangle \tag{9}$$

where $\mathbf{F}_B^X$ is the first-order Kohn−Sham (KS) operator. $\mathbf{F}_B^X$ can be decomposed as follows:

$$\mathbf{F}_B^X = \mathbf{h}_B^X + \tilde{\boldsymbol{F}}_B^X \tag{10a}$$

$$\tilde{\mathbf{F}}_B^X = \sum_{l}^{occ}\sum_{\sigma}\int \mathrm{d}^3r\,\frac{\delta F}{\delta\psi_{l\sigma}(\mathbf{r})}\vec{\psi}_{l\sigma}^{(B),X} = \tilde{F}_l^{(B),X} \tag{10b}$$

$\tilde{\mathbf{F}}_B^X$ describes the change of the KS operator due to the first-order changes of the KS orbitals, i.e., the feedback of the orbitals on the KS operator. With the definitions

$$Z_{AB}^{X,k} = \sum_{\sigma}^{occ}\sum_{a\sigma'}^{virt}\langle\psi_{k\sigma}^{(0)}|\mathbf{h}_A^X|\psi_{a\sigma'}^{(0)}\rangle\frac{\langle\psi_{a\sigma'}^{(0)}|\mathbf{h}_B^X|\psi_{k\sigma}^{(0)}\rangle}{\epsilon_k - \epsilon_a} \tag{11a}$$

$$\tilde{Z}_{AB}^{X,k} = \sum_{\sigma}^{occ}\sum_{a\sigma'}^{virt}\langle\psi_{k\sigma}^{(0)}|\mathbf{h}_A^X|\psi_{a\sigma'}^{(0)}\rangle\frac{\langle\psi_{a\sigma'}^{(0)}|\tilde{\mathbf{F}}_B^X|\psi_{k\sigma}^{(0)}\rangle}{\epsilon_k - \epsilon_a} \tag{11b}$$

one can represent K_{AB}^X as

$$K_{AB}^X = C\sum_{k}^{occ}(Z_{AB}^{X,k} + \tilde{Z}_{AB}^{X,k}) \tag{12}$$

($C = -2/3$ for X = PSO, $C = 2/3$ for X = FC and X = SD). Equations 9−12 are given for canonical zeroth-order orbitals; however, the extension to localized orbitals is straightforward.

With the help of the $\tilde{F}_{l\sigma}^{(B),X}$ introduced in eq 10b, $\tilde{Z}_{AB}^X$ can be represented as

$$\tilde{Z}_{AB}^{X,k} = \sum_{l}^{occ}\tilde{Z}_{AB}^{X,kl} \tag{13a}$$

$$\tilde{Z}_{AB}^{X,kl} = \sum_{\sigma}^{occ}\sum_{a\sigma'}^{virt}\langle\psi_{k\sigma}^{(0)}|\mathbf{h}_A^X|\psi_{a\sigma'}^{(0)}\rangle\frac{\langle\psi_{a\sigma'}^{(0)}|\tilde{\mathbf{F}}_l^{(B),X}|\psi_{k\sigma}^{(0)}\rangle}{\epsilon_k - \epsilon_a} \tag{13b}$$

From eq 13b, it is obvious that $\tilde{Z}_{AB}^{X,k}$ is the self-consistent response of occupied orbital k to the perturbation by the spin angular momentum of nucleus B. If one separates the self-interaction term $\tilde{Z}_{AB}^{X,kk}$ from the genuine interaction terms $\tilde{Z}_{AB}^{X,kl}$

where $l \neq k$, K_{AB}^{X} can be decomposed into[20]

$$K_{AB}{}^{X} = C\sum_{k}^{occ}(Z_{AB}^{X,k} + \tilde{Z}_{AB}^{X,kk}) + C\sum_{k}^{occ}\sum_{l,l\neq k}^{occ}\tilde{Z}_{AB}^{X,kl} = \sum_{k}^{occ}K_{A,B}^{X,k} + \sum_{k}^{occ}\sum_{l,l\neq k}^{occ}K_{A,B}^{X,kl} \quad (14)$$

Here, $K_{AB}^{X,k}$ covers all processes where the perturbing spin modifies orbital k directly. Term $K_{AB}^{X,kl}$ describes such processes where the perturbation changes the shape of orbital l, which in turn changes the first-order KS operator and eventually orbital k. For magnetic perturbations, this interaction between orbitals l and k is mediated exclusively by the XC potential. The interaction is closely related to the concept of steric exchange repulsion: If two molecules or two molecular groups approach each other, steric repulsion (exchange repulsion) will hinder them to penetrate each other. Suppose that orbital k belongs to the first molecule (molecular group) and orbital l to the second. Then exchange repulsion leads to distortions of the orbitals; i.e., they become polarized. Due to the Pauli principle (i.e., the antisymmetry of the wave function), the shape of orbital k is subjected to the constraint that it has to be orthogonal to orbital l if k and l are of the same spin. Thus, if orbital l is polarized, the constraint for k is modified as well and eventually orbital k will undergo a change in addition to the change caused by the perturbation directly. The same applies in the case of a magnetic perturbation, and therefore, it is justified to relate the two-orbital terms to steric exchange effects. We note, however, that in the case of steric repulsion, one considers the interaction between occupied zeroth-order orbitals whereas in the case of the magnetic perturbation, a zeroth-order and a first-order orbital are considered.

We will use the shorthand notation ($k \leftarrow l$) for the corresponding contribution to remind us of this. Thus, though $K_{AB}^{X,k}$ is dominated by one-particle effects, $K_{AB}^{X,kl}$ accounts for the steric exchange effects between orbitals k and l. The first-order orbital $\psi_k^{(B),X}$ depends on which nucleus B is perturbed. When the perturbing and responding orbital switch their roles, then the corresponding two-orbital terms $K_{AB}^{X,k\leftarrow l}$ and $K_{AB}^{X,\leftarrow k}$ are not identical. However, their sum is independent of the nucleus perturbed and therefore it is better to discuss the combination term (k,l), i.e., $K_{A,B}^{X,(k,l)}$, when describing the interaction between orbitals k and l in connection with the coupling mechanism.

Because the perturbations are linearly dependent on the occupied MOs, one can calculate each orbital contribution $K_{AB}^{X,k}$ or $K_{AB}^{X,kl}$ separately in a consistent manner by restricting orbital relaxation to certain orbital sets. The sum of all orbital contributions, evaluated separately for the FC, PSO, DSO, and SD terms, will lead to the total indirect scalar SSCC.[20]

The reduced SSCCs of the twelve hydrides investigated in this work were determined by CPDFT using the procedure recently described by Sychrovský, Gräfenstein, and Cremer.[18] All calculations were carried out with the B3LYP hybrid functional[22−24] and Pople's 6-311G(d,p) basis[25] at B3LYP/6-31G(d,p) geometries determined in this work. Actually, the 6-311G(d,p) basis set is not suited for SSCC calculations because it was optimized for energy calculations. Nevertheless it was used in this work because (a) the determination of qualitative trends rather than high accuracy of the calculated SSCCs is the goal of this work and (b) the 6-311G(d,p) basis is defined for all atoms X considered. In some cases calculated SSCCs were improved by using Dunning's cc-pVQZ basis set,[26]

SCHEME 1: One- and Two-Orbital Contributions to SSCCs ^1K(X1H2)[a]

one-orbital contributions	two-orbital contributions				sum of two-orbital contributions
bd	bd<—lp	+	lp<—bd	=	bd,lp
lp	bd<—ob	+	ob<—ld	=	bd,ob
ob	bd<—c	+	c<—bd	=	bd,c
c	lp<—ob	+	ob<—lp	=	lp,ob
	lp<—c	+	c<—lp	=	lp,c
	ob<—c	+	c<—ob	=	ob,c

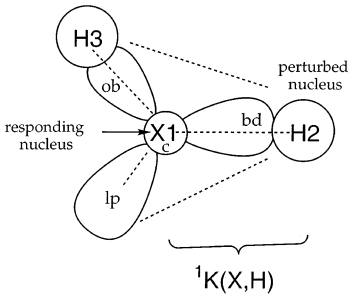

[a] Abbreviations: bd, lp, ob, and c denote bond, lone pair, other bond, and core LMO. The symbol ← points from the perturbed occupied orbital to the responding occupied orbital.

which corresponds to a (12s6p3d2f1g/6s3p2d1f) [5s4p3d2f1g/4s3p2d1f] contraction where the g-type polarization functions were deleted because of computational limitations.

A better understanding of the calculated SSCCs is obtained by analysis of zeroth-order and first-order orbitals, the Fermi contact spin density distribution, and the spin density at the position of the coupling nuclei. As zeroth-order orbitals, Boys' localized MOs[27] were used. The localization of core and valence orbitals was carried out separately to avoid core orbitals with long valence tails, which lead to artificially exaggerated core orbital contributions. If X1 and H2 are the coupling nuclei, we will distinguish in this work between X1−H2 bond (bd), X1 lone pair (lp), X1 core (c), and X1−H3, X1−H4, etc., other bond (ob) orbitals (see Scheme 1). In this way the constant ^1K(X1H2) = ^1K(XH) has sixteen different orbital contributions, which comprise four one-orbital and twelve two-orbital contributions $x-y$, where the latter are contracted to six two-orbital values (k, l) = ($k \leftarrow l$) + ($l \leftarrow k$), as indicated in Scheme 1. The program J-**OC**-PSP is set up such a way that with each one-orbital calculation all corresponding two-orbital contributions are obtained and the actual calculation of the one-orbital contributions is handled as a calculation of four different SSCCs. In this way, one single run leads to all orbital contributions.

According to eqs 3 and 7, the FC term is proportional to the spin density at the responding nucleus:

$$K_{AB}^{FC} = \frac{8}{3}\pi\alpha^2\rho^{(B),FC}(\mathbf{R}_A) \quad (15)$$

where the first-order density, called here the *Fermi contact spin density distribution*

$$\rho^{(B),FC}(\mathbf{r}) = 2\sum_{k}^{occ}\sum_{\sigma}\psi_{k\sigma}^{(0)}(\mathbf{r})\,\psi_{k\sigma}^{(B),FC}(\mathbf{r}) \quad (16)$$

can be taken for an arbitrary orientation of the perturbing nuclear

TABLE 1: FC Orbital Contributions to the One-Bond Coupling Constants ^1K(XH) in XH_n Molecules[a]

type	$^1K^{FC}$(bd)	$^1K^{FC}$(lp)	$^1K^{FC}$(ob)	$^1K^{FC}$(c)	$^1K^{FC}$(bd,lp)	$^1K^{FC}$(bd,ob)	$^1K^{FC}$(bd,c)	$^1K^{FC}$(lp,ob)	$^1K^{FC}$(lp,c)	$^1K^{FC}$(ob,c)	total
CH_4	52.10		−3.43	−0.04		−7.43	−2.36			−0.36	38.48
SiH_4	116.08		−12.58	−0.09		−27.34	2.81			−0.59	78.30
GeH_4	322.74		−37.87	−0.02		−96.20	6.77			−1.15	194.27
NH_3	79.15	−5.16	−4.94	−0.03	−16.35	−9.66	−5.75	2.29	−0.40	−0.33	38.83
PH_3	96.37	−19.31	−5.28	−0.04	−34.56	−12.86	−0.40	3.40	−0.80	−0.17	26.35
AsH_3	207.47	−52.09	−10.66	−0.02	−98.45	−31.92	2.20	7.92	−1.23	−0.16	23.04
OH_2	115.31	−23.98	−5.59	−0.02	−41.92	−10.43	−9.64	4.86	−1.95	−0.29	26.34
SH_2	134.75	−38.86	−5.25	−0.03	−65.06	−12.71	−1.31	4.47	−1.55	−0.14	14.32
SeH_2	266.51	−86.41	−9.85	0.00	−155.20	−27.28	1.96	9.00	−1.85	−0.12	−3.21
FH	157.73	−55.38		−0.01	−76.45		−12.73		−5.08		8.08
ClH	181.85	−70.43		−0.02	−109.76		−1.73		−2.71		−2.78
BrH	333.73	−137.44		−0.02	−234.44		1.66		−2.71		−39.22

[a] All K values in SI units [10^{19} kg m^{-2} s^{-2} Å^{-2}] calculated at the CP-DFT/B3LYP/6-311G(d,p) level of theory. The following isotopes are used in the calculations: ^{13}C; ^{29}Si; ^{73}Ge; ^{15}N; ^{31}P; ^{75}As; ^{17}O; ^{33}S; ^{77}Se; ^{19}F; ^{35}Cl; ^{81}Br.

TABLE 2: PSO Orbital Contributions to the One-Bond Coupling Constants ^1K(XH) in XH_n Molecules[a]

type	$^1K^{PSO}$(bd)	$^1K^{PSO}$(lp)	$^1K^{PSO}$(ob)	$^1K^{PSO}$(c)	$^1K^{PSO}$(bd,lp)	$^1K^{PSO}$(bd,ob)	$^1K^{PSO}$(bd,c)	$^1K^{PSO}$(lp,ob)	$^1K^{PSO}$(lp,c)	$^1K^{PSO}$(ob,c)	total
CH_4	−0.19		0.64	0.00		0.08	0.00			0.00	0.54
SiH_4	−0.07		−0.04	−0.03		0.01	0.00			0.00	−0.13
GeH_4	0.37		−0.64	−0.22		−0.03	0.01			−0.03	−0.54
NH_3	−0.73	1.29	1.67	0.00	0.04	0.16	0.00	0.05	0.00	0.00	2.47
PH_3	−0.34	0.32	0.97	0.23	−0.08	0.07	−0.01	0.01	0.01	0.03	1.21
AsH_3	−0.10	0.06	1.95	0.22	−0.30	0.12	0.01	0.13	0.00	0.03	2.12
OH_2	−2.13	7.01	2.22	0.01	0.09	0.22	−0.01	0.32	0.01	0.00	7.74
SH_2	−1.27	4.08	1.38	0.45	−0.08	0.13	−0.03	0.11	0.08	0.03	4.89
SeH_2	−1.59	6.70	2.39	0.67	−0.33	0.22	−0.02	0.27	0.10	0.04	8.46
FH	−5.06	23.68		0.01	0.09		−0.01		0.00		18.72
ClH	−2.26	14.22		0.82	−0.03		−0.02		0.12		12.86
BrH	−4.32	24.88		1.26	−0.21		−0.06		0.35		21.90

[a] All K values in SI units [10^{19} kg m^{-2} s^{-2} Å^{-2}] calculated at the CP-DFT/B3LYP/6-311G(d,p) level of theory. The following isotopes are used in the calculations: ^{13}C; ^{29}Si; ^{73}Ge; ^{15}N; ^{31}P; ^{75}As; ^{17}O; ^{33}S; ^{77}Se; ^{19}F; ^{35}Cl; ^{81}Br.

spin at B. As the FC term is isotropic, we will orient the nuclear spin toward the positive z axis. One can split $\rho^{(B),FC}$ into one- and two-orbital contributions in the same way as K_{AB}^{FC}:

$$K_{AB}^{FC,k} = \frac{8}{3}\pi\alpha^2\rho_k^{(B),FC}(\mathbf{R}_A) \tag{17a}$$

$$K_{AB}^{FC,kl} = \frac{8}{3}\pi\alpha^2\rho_{kl}^{(B),FC}(\mathbf{R}_A) \tag{17b}$$

where

$$\rho_k^{(B),FC}(\mathbf{r}) = 2\sum_{\sigma}^{occ}\sum_{a\sigma'}^{virt}\frac{\langle\psi_{a\sigma'}^{(0)}|h_{k,z}^{(B),FC} + \tilde{F}_{k,z}^{(B),FC}|\psi_{k\sigma}^{(0)}\rangle}{\epsilon_k - \epsilon_a}\psi_{a\sigma'}^{(0)}(\mathbf{r})\,\psi_{k\sigma}^{(0)}(\mathbf{r}) \tag{18a}$$

$$\rho_{kl}^{(B),FC}(\mathbf{r}) = 2\sum_{\sigma}^{occ}\sum_{a\sigma'}^{virt}\frac{\langle\psi_{a\sigma'}^{(0)}|\tilde{F}_{l,z}^{(B),FC}|\psi_{k\sigma}^{(0)}\rangle}{\epsilon_k - \epsilon_a}\psi_{a\sigma'}^{(0)}(\mathbf{r})\,\psi_{k\sigma}^{(0)}(\mathbf{r}) \tag{18b}$$

It should be noted that the FC perturbation leads to opposite changes in corresponding α and β orbitals (we consider closed-shell systems). Thus, the change of the total density vanishes in first order, and the changes in the spin density are just twice the change of the α-spin density. In the following, by the spin density of an orbital we mean the spin density of a pair of corresponding α and β orbitals.

For the analysis of the FC term, also the s-density at nucleus $X1$ and nucleus $H2$ was calculated according to

$$\varrho_s^l(N) = \langle\phi_l|\delta(\mathbf{r}_N)|\phi_l\rangle \tag{19}$$

where $\delta(\mathbf{r}_N)$ is the Dirac delta function and ϕ_l is the localized bond or lone pair orbital. The product $\varrho_s^{(ll')}(X,H) = \varrho_s^l(X)\,\varrho_s^{l'}(H)$ can be related to the magnitude of the FC term.

Calculations were carried out with COLOGNE 2003[28] (all SSCC calculations) and Gaussian 98[29] (geometry optimizations).

3. Results and Discussions

In Tables 1−5, the FC, PSO, SD, DSO, and total orbital contributions to ^1K(XH) of the twelve XH_n hydrides investigated are listed. In Table 6, the bond orbital or lone pair orbital density at the coupling nuclei calculated according to eq 19 are given together with atom polarizability and electronegativity of atom X of molecules XH_n,[30] which are used for the analysis of the calculated orbital contributions. Spin density distributions, zeroth-order and first-order bond orbitals (perturbation at H2) are shown in Figures 1−5.

3.1. Sign of the Orbital Contributions to the Fermi Contact Term. In the following we will discuss the various orbital contributions to the FC term. They are schematically indicated in Figure 5.

Bond Orbital Contribution. The bond orbital contribution to ^1K(XH) is always positive, which can be understood by inspection of the zeroth- and first-order localized XH bond orbital (example CH_4: see Figure 1a,b, perturbation at H2). The bond orbital is formed in zeroth order from a hybrid orbital and the hydrogen 1s orbital (Figure 1a). At H2, the bond orbital has a positive sign and the atom C is located in the negative lobe of the bond orbital. For the case that the magnetic perturbation is at H2, the first-order localized C−H2 bond orbital is dominated by an admixture of the σ^*(C−H2) orbital. This leads to an additional nodal plane in the C−H2 bond region and a sign reversion at H2 (see Figure 1b). The sign of the spin density at C and H2 can be assessed from the corresponding signs of zeroth- and first-order orbital (C: -, -; H2: +, -). Hence a positive sign results for C (dominance of α-spin density) and a negative sign for H2 (dominance of β-spin density, see Figure 1c), which is in line with the Dirac model shown in Figure 5a.

Assuming that at H2 the nucleus adopts α-spin, then Fermi coupling will lead to a dominance of β-spin density at the H2

TABLE 3: SD Orbital Contributions to the One-Bond Coupling Constants ^1K(XH) in XH_n Molecules[a]

type	$^1K^{SD}$(bd)	$^1K^{SD}$(lp)	$^1K^{SD}$(ob)	$^1K^{SD}$(c)	$^1K^{SD}$(bd,lp)	$^1K^{SD}$(bd,ob)	$^1K^{SD}$(bd,c)	$^1K^{SD}$(lp,ob)	$^1K^{SD}$(lp,c)	$^1K^{SD}$(ob,c)	total
CH_4	−0.22		0.27	0.00		0.02	0.00			0.00	0.06
SiH_4	−0.09		0.08	−0.02		0.02	−0.01			0.00	−0.01
GeH_4	−0.20		0.22	0.00		0.03	0.00			0.00	0.06
NH_3	−0.75	0.31	0.50	0.00	−0.01	0.02	0.00	0.13	0.00	0.00	0.19
PH_3	−0.52	−0.03	0.33	−0.01	−0.04	0.03	−0.02	0.06	0.00	0.01	−0.20
AsH_3	−0.88	−0.08	0.63	−0.01	−0.15	0.04	−0.01	0.10	0.00	0.01	−0.35
OH_2	−1.76	1.50	0.47	0.00	−0.19	−0.02	0.00	0.23	0.00	0.00	0.22
SH_2	−1.19	0.76	0.31	−0.01	−0.10	0.02	−0.04	0.09	0.02	0.01	−0.12
SeH_2	−1.83	1.22	0.52	−0.01	−0.30	0.02	−0.03	0.14	0.02	0.01	−0.24
FH	−3.07	3.53		0.00	−0.92		0.00		0.00		−0.46
ClH	−2.27	2.46		−0.01	−0.28		−0.01		0.01		−0.11
BrH	−3.03	4.08		−0.01	−0.57		−0.05		0.07		0.48

[a] All K values in SI units [10^{19} kg m^{-2} s^{-2} Å^{-2}] calculated at the CP-DFT/B3LYP/6-311G(d,p) level of theory. The following isotopes are used in the calculations: ^{13}C; ^{29}Si; ^{73}Ge; ^{15}N; ^{31}P; ^{75}As; ^{17}O; ^{33}S; ^{77}Se; ^{19}F; ^{35}Cl; ^{81}Br.

TABLE 4: DSO Orbital Contributions to the One-Bond Coupling Constants ^1K(XH) in XH_n Molecules[a]

type	$^1K^{DSO}$(bd)	$^1K^{DSO}$(lp)	$^1K^{DSO}$(ob)	$^1K^{DSO}$(c)	total
CH_4	−0.33		0.43	0.02	0.11
SiH_4	−0.07		0.11	0.00	0.04
GeH_4	−0.13		0.11	0.00	−0.02
NH_3	−0.58	0.21	0.43	0.00	0.05
PH_3	−0.12	0.05	0.09	0.00	0.01
AsH_3	−0.16	0.07	0.08	−0.01	−0.01
OH_2	−0.87	0.61	0.29	−0.02	0.00
SH_2	−0.19	0.14	0.06	−0.01	0.01
SeH_2	−0.20	0.14	0.05	−0.01	−0.01
FH	−1.20	1.24		−0.05	−0.01
ClH	−0.31	0.36		−0.01	0.03
BrH	−0.24	0.24		−0.01	−0.01

[a] All K values in SI units [10^{19} kg m^{-2} s^{-2} Å^{-2}] calculated at the CP-DFT/B3LYP/6-311G(d,p) level of theory. The following isotopes are used in the calculations: ^{13}C; ^{29}Si; ^{73}Ge; ^{15}N; ^{31}P; ^{75}As; ^{17}O; ^{33}S; ^{77}Se; ^{19}F; ^{35}Cl; ^{81}Br.

nucleus (i.e., the bond electron next to the H2 nucleus possesses preferably β-spin). Pauli coupling (or electron pair coupling) will imply that the bonding electron close to the X nucleus will adopt preferably α spin, which in turn will lead to β-spin for the spin moment of nucleus X via Fermi coupling. According to the definition of the sign for SSCCs, this leads to a positive ^1K(XH, bond) contribution as predicted by the Dirac model for a one-bond NMR spin−spin coupling mechanism (Figure 5a).

For SiH_4 the situation is slightly complicated by an extra-nodal plane both in the zeroth- and first-order orbitals (Figure 1d,e, perturbation again at H2) but otherwise the orbitals closely resemble those of CH_4. The signs of the zeroth-order Si−H2 bond orbital at Si and H2 are both positive; however, the corresponding signs of the first-order orbital (Figure 1e) are positive and negative so that again the spin density is positive at the heavy atom (Si) and negative at H2. Obviously, the same sign relationships as observed for the first period atom C are preserved for the second period atom Si by addition of another nodal plane between X and H2.

Another regularity of the hybrid orbitals used to establish bond and lone pair orbitals becomes obvious by inspection of Figure 2 showing LMOs and spin density distribution of FH and Figure 3 showing the same for H_2X (X = O and Se). The X−H2 bond orbital has always H2 in the front lobe whereas X and other nuclei such as H3, H4, etc. are located in the back lobe of the hybrid orbital forming the bond orbital. The first-order orbital gets an additional nodal plane so that the resulting spin density distribution complies with the Dirac model irrespective of the group or period atom X belongs to. All zeroth-order bond orbitals, all first-order bond orbitals, and consequently all spin density distribution associated with bond X−H2 resemble each other. This, however, will only be true if the perturbation is at H2 rather than X. The first-order orbitals have a larger admixture from other XH_n orbitals in the latter case, which makes the analysis somewhat more difficult. However, again the same sign relationships for orbitals and spin density result. This reflects the fact that the SSCC in reality as well as in the CPDFT method is independent of the nucleus perturbed.[18] We can conclude that the Dirac model applies to the contribution of the bond orbital and can be recovered by inspection of the nodal structure of zero- and first-order bond orbital.

Lone Pair, Other Bond, and Core Orbital Contributions. In the case of the lone pair orbitals, X and H2, H3, etc. are always positioned in its back lobe, accordingly the sign of the zeroth-order orbital is identical at X and H2 (see Figures 2d,e, and 4). If the perturbation is at H2, the first-order lone pair orbital resembles closely the first-order bond orbital because again the σ^*(X−H2) orbital makes the largest contribution to this orbital. Just another nodal plane is added and atom X is shifted into the back lobe of the orbital in the same way as in the case of the first-order bond orbital. One can say that the sign relationships of the first-order orbital at the X and H2 nuclei are retained no matter whether a bond, lone pair, or core orbital is expected. Hence, the sign of the spin density distribution at the nuclei considered (Figure 2f) is determined by the corresponding signs of the zeroth-order orbital. These are equal for lone pair orbitals, other bond orbitals, and the core orbitals, which means that the corresponding spin density distributions have negative signs both at X and H2, thus leading to negative lone pair, other bond, and core orbital contributions to ^1K(XH). This is confirmed by the results of the J-**OC**-PSP calculations (see Table 1) and can be considered to be generally true.

One can translate the spin density contribution obtained for a particular LMO into an extended Dirac model focusing just on the situation at the nuclei, which is relevant for Fermi coupling. Taking again the preferred spin of H2 as α (Figure 5b), Fermi coupling will lead to a dominance of β-spin at nucleus H2 as well as in the whole back lobe of the lone pair orbital, which encompasses the XH bonds, e.g., in XH_2 or XH_3. Orbital relaxation in the electron lone pair will imply a preference of α-spin in the front lobe (see Figures 2f and 6b). Because X is located in the back lobe, β spin density is found at X and Fermi coupling yields a preference for α spin for nucleus X. An unfavorable interaction between the α spin of nucleus H2 and nucleus X results and a negative contribution to ^1K(XH) is the consequence (see Figure 5b). The same line of arguments applies to the other bond orbital contributions and the core orbital contributions, which are schematically indicated in Figure 5c,d, respectively. We note in this connection that the extended Dirac models give only the preferred spin at the nuclei; however, they do not provide a model for the spin density

TABLE 5: Total Orbital Contributions to the One-Bond Coupling Constants ^1K(XH) in XH_n Molecules[a]

type	^1K(bd)	^1K(lp)	^1K(ob)	^1K(c)	^1K(bd,lp)	^1K (bd,ob)	^1K(bd,c)	^1K(lp,ob)	^1K(lp,c)	^1K(ob,c)	total[b]		exp[c]
CH_4	51.36		−2.10	−0.02		−7.33	−2.36			−0.36	39.19		41.3
SiH_4	115.84		−12.42	−0.14		−27.3	2.80			−0.59	78.20		84.9
GeH_4	322.79		−38.18	−0.24		−96.2	6.79			−1.18	193.77		232
NH_3	77.09	−3.36	−2.35	−0.02	−16.32	−9.48	−5.76	2.47	−0.39	−0.33	41.54	46.33	50
PH_3	95.39	−19.00	−3.89	0.17	−34.67	−12.76	−0.43	3.46	−0.80	−0.43	27.37	32.01	37.8
AsH_3	206.32	−52.04	−7.99	0.19	−98.90	−31.76	2.20	8.15	−1.23	−0.12	24.80	33.11	45
OH_2	110.54	−14.86	−2.62	−0.04	−42.01	−10.24	−9.64	5.41	−0.39	−0.29	34.31		48
SH_2	132.10	−33.88	−3.49	0.40	−65.24	−12.56	−1.38	4.67	−1.44	−0.10	19.08		
SeH_2	262.90	−78.34	−6.88	0.65	−155.83	−27.05	1.91	9.41	−1.73	−0.07	5.00		28.4
FH	146.40	−26.93		−0.05	−77.28		−12.74		−5.08		26.33		46.9
ClH	177.01	−53.39		0.77	−110.07		−1.76		−2.58		10.00	16.43	32
BrH	326.13	−108.24		1.22	−235.23		1.54		−2.29		−16.86	−7.67	(±)19[d]

[a] All K values in SI units [10^{19} kg m^{-2} s^{-2} Å^{-2}] calculated at the CP-DFT/B3LYP/6-311G(d,p) level of theory. The following isotopes are used in the calculations: ^{13}C; ^{29}Si; ^{73}Ge; ^{15}N; ^{31}P; ^{75}As; ^{17}O; ^{33}S; ^{77}Se; ^{19}F; ^{35}Cl; ^{81}Br. [b] Second entry corresponds to total ^1K(XH) values obtained with Dunning's cc-pV5Z basis set. [c] Taken fromr ref 3b. [d] Sign uncertain.

TABLE 6: s-Density at Nuclei X and H As Given by Bond and Lone Pair LMO of XH_n, Polarizability α(X), and Electronegativity χ(X)[a]

	XH bond		lone pair			χ(X)	
type	X	H	X	H	α_X	Pauling	Allred-Rochow
CH_4	0.516	0.217			1.76	2.55	2.50
SiH_4	0.779	0.197			5.38	1.90	1.74
GeH_4	2.035	0.188			6.07	2.01	2.02
NH_3	0.814	0.217	1.566	0.000	1.10	3.04	3.07
PH_3	0.795	0.194	3.265	0.003	3.63	2.19	2.06
AsH_3	1.658	0.185	8.074	0.004	4.31	2.18	2.20
OH_2	1.469	0.208	3.949	0.004	0.80	3.44	3.50
SH_2	1.353	0.186	5.511	0.006	2.90	3.44	3.50
SeH_2	2.549	0.179	11.797	0.007	3.77	2.55	2.48
FH	2.903	0.186	7.850	0.015	0.56	3.98	4.10
ClH	2.434	0.172	8.902	0.013	2.18	3.16	2.83
BrH	4.088	0.167	17.109	0.013	3.05	2.96	2.74

[a] The s-density is given in e/a_0^3; the polarizability, in Å^3.[30] See text for the calculation of the *s*-density at the nucleus.

distribution in the total molecule, which is much more complicated, as can be seen from Figures 1 and 2.

Similarly to the case of the bond orbital contributions, the same sign relationships are retained when X is a second or third period atom. Additional nodal planes enter the zeroth-order and first-order orbitals (Figures 3−5). The sign of the spin density distribution at the coupling nuclei is quickly determined by inspection of the phase of the zeroth-order orbitals at these nuclei (Figures 3−5).

Two-Orbital Interaction Contributions. Two-orbital interaction terms account for a considerable portion of the total FC terms. If an orbital *l* gets an α surplus density in some region, this leads to an extra exchange potential in this region that is α-attractive and β-repulsive. This extra potential will enhance the α density of the other electrons in this region, leading to an increased β density in other regions.

The interaction contributions (*k*, *l*) are always made up from (k ← l) and (l ← k), where both can have the same or opposite signs. In the latter case a sign prediction will only be possible if the relative magnitude of the two contributions can be estimated.

We consider first the (bd,lp) contribution. If the nucleus at H2 has an α spin the bd orbital will have a β surplus spin density around H2 and an α surplus spin density at X. This α surplus spin density is concentrated in the valence region of X. The corresponding extra exchange potential attracts α density from the lp orbital, which is withdrawn among others from the inner core region. The spin density of the lp orbitals at X is shifted toward the β spin, and the (lp ← bd) contribution to the FC term is negative. The lp terms, in contrast, have a surplus β density in the valence region, and the spin density of the bd orbital at X is shifted toward α, i.e., the (bd ← lp) term is positive, and the sign of the (bd,lp) contribution is not evident. However, the bd orbital responds much more strongly by the nuclear spin at H2 than the lp orbital. Hence, the (lp ← bd) effect is stronger than the (bd ← lp) term, and (bd,lp) is negative. The argument holds in full analogy for the (bd,ob) term. As regards the (lp,ob) term, the lp and ob orbitals both attract β density in the valence region of X and shift thus the spin density of each other at X toward α, which accounts for the positive sign of the (lp,ob) contributions.

The (bd,c) contributions become more positive as the size of the core increases. Although they are negative for all second-row X atoms, they are positive for X in the fourth row. Besides, the (bd,c) contributions become more negative with increasing electronegativity of X. One has to keep in mind that the direct response of the c orbital to the nuclear spin at H2 is negligible; i.e., c responds to the nuclear spin only by mediation of the other orbitals, above all the bd orbital. The results give at hand that the details of this response, and the feedback of the perturbed c orbital to the bd orbital, depend on the size and structure of the core at X.

3.2. Magnitude of the Orbital Contributions to the Fermi Contact Term. All FC contributions except those for H_2Se, HCl, and HBr are calculated to be positive. The FC terms increase with increasing atomic number in group IV but decrease in groups V, VI, and VII of the periodic table. Within a period of the periodic table a decrease is found (exception CH_4 and NH_3: 38.5 and 38.8 SI units, Table 1) The calculated trends in the FC contributions can be explained by comparing the positive bond contributions with the negative lp, (b,lp), ob, and (b,ob) contributions. Among the negative contributions the lp and (b,-lp) contributions play the strongest role reducing the positive bond orbital contributions. Together with the other negative orbital contributions, they annihilate the effect of the positive bond contributions and lead to a decrease of the FC term within a group. They become even negative for SeH_2 (−3.2), ClH (−2.8), and BrH (−39.9 SI units, Table 1). However, in group IV where no lone pair contributions exist, the FC term increases with increasing atomic number. For the purpose of explaining these trends, in Table 6 we have listed the bond orbital or lone pair orbital density at the coupling nuclei calculated according to eq 19 together with atom polarizability and electronegativity of atom X of molecules XH_n.[30]

The bond orbital contributions to the FC term increase in the first period with increasing electronegativity but possess a minimum for second and third period atoms X in group V (PH_3 and AsH_3, Table 1, second column). These trends reflect the influence of two opposing effects, namely electronegativity and polarizability. In the first period the polarizability plays only a

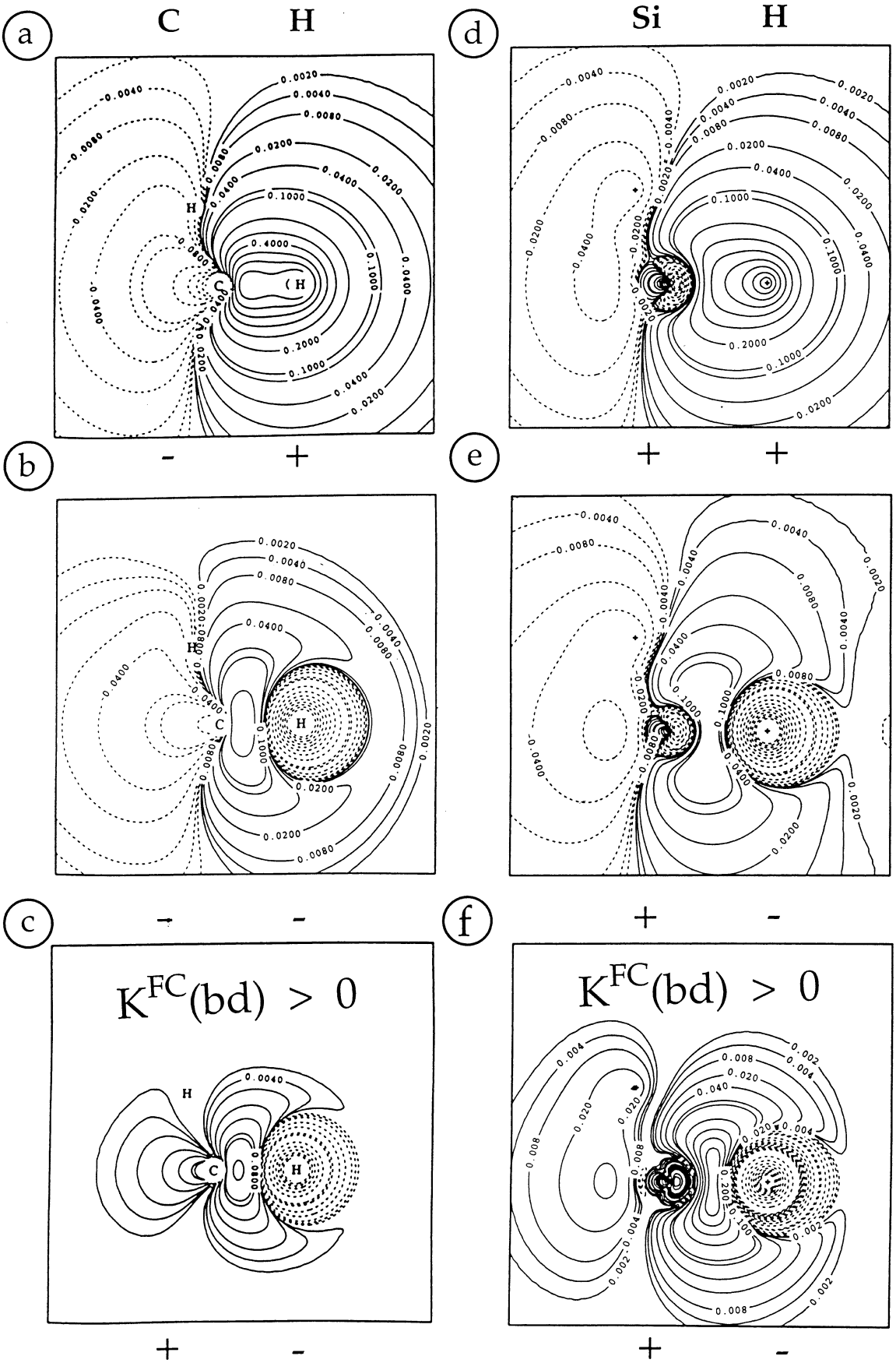

Figure 1. Contour line diagram of (a) the C−H2 bonding LMO of CH_4, (b) the first-order C−H2 bonding LMO (perturbation at H2), (c) the FC spin density distribution of the bonding C−H2 orbital, (d) the Si−H2 bonding LMO of SiH_4, (e) the first-order Si−H2 bonding LMO (perturbation at H2), and (f) the FC spin density distribution of the bonding Si−H2 orbital. H2 is located at the right and H3 at the upper left of the C(Si) atom. Solid contour lines indicate the positive orbital phase (spin density distribution, i.e., more α-density), dashed contour lines the negative orbital phase (spin density distribution, i.e., more β-density). B3LYP/6-311G(d,p) calculations.

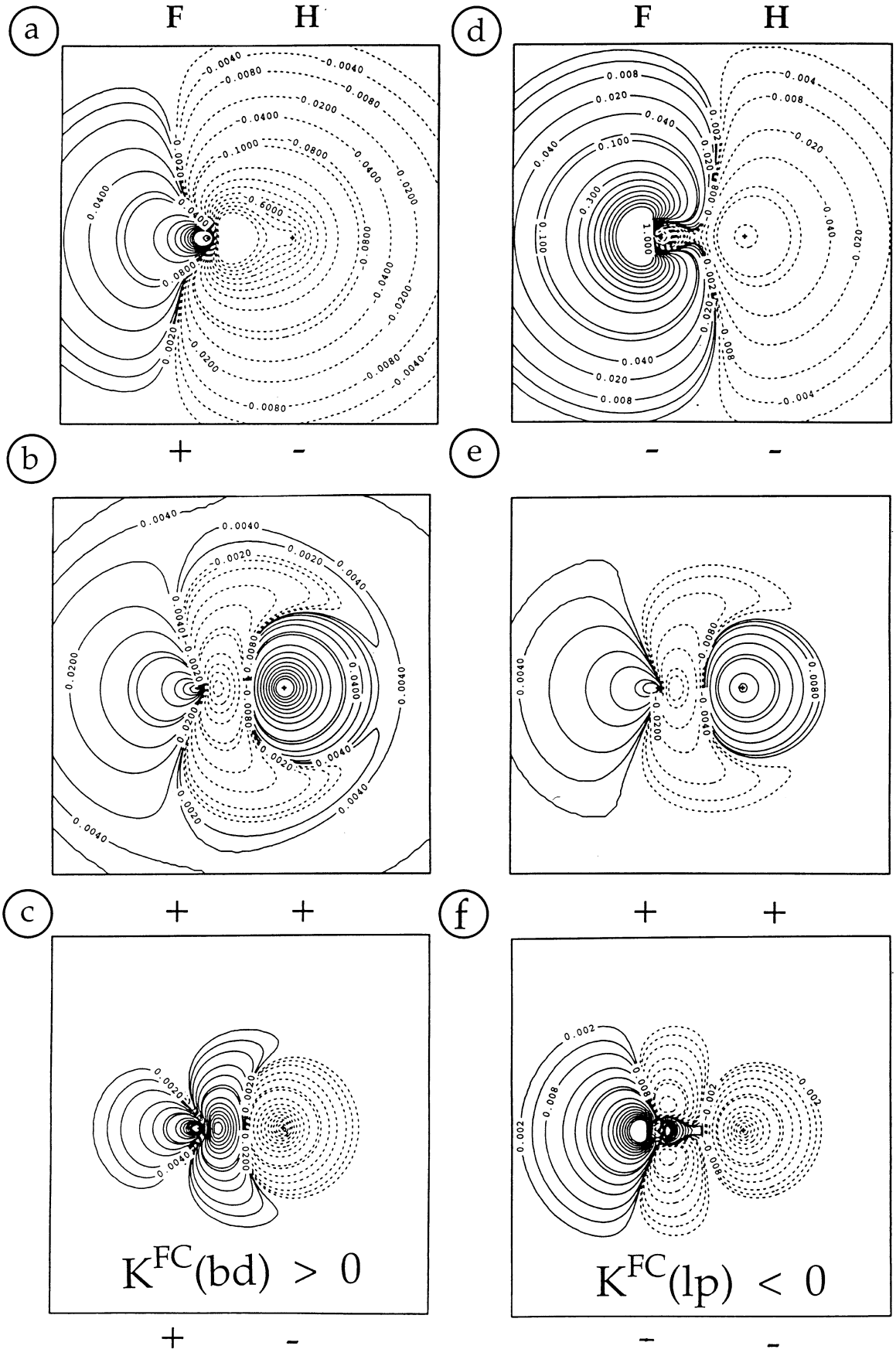

Figure 2. Contour line diagram of (a) the F−H2 bonding LMO of FH, (b) the first-order F−H2 bonding LMO, (c) the FC spin density distribution of the bonding FH orbital, (d) the F lone pair LMO of FH, (e) the first-order F lone pair LMO, and (f) the FC spin density distribution of the lone pair orbital of F in FH. The perturbation is always at H2. Solid contour lines indicate the positive orbital phase (spin density distribution, i.e., more α-density); dashed contour lines, the negative orbital phase (spin density distribution, i.e., more β-density). The sign of orbital and spin density at the coupling nuclei are given below each diagram. B3LYP/6-311G(d,p) calculations.

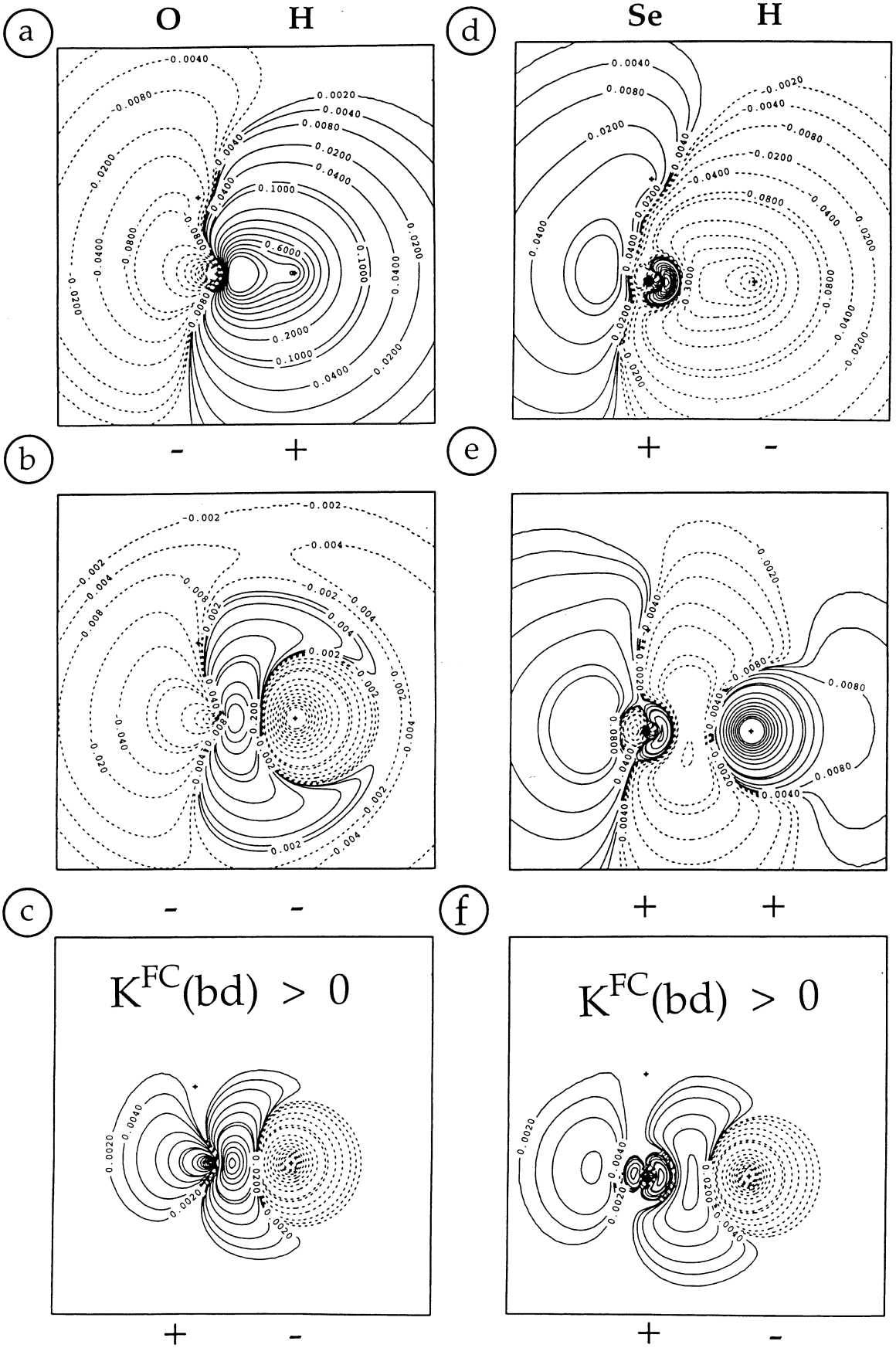

Figure 3. Contour line diagram of (a) the O−H2 bonding LMO of OH_2, (b) the first-order O−H2 bonding LMO, (c) the FC spin density distribution of the bonding O−H2 orbital, (d) the Se−H2 bonding LMO of SeH_2, (e) the first-order Se−H2 bonding LMO, and (f) the FC spin density distribution of the bonding Se−H2 orbital. The perturbation is always at H2. Solid contour lines indicate the positive orbital phase (spin density distribution, i.e., more α-density); dashed contour lines, the negative orbital phase (spin density distribution, i.e., more β-density). The sign of orbital and spin density at the coupling nuclei are given below each diagram. B3LYP/6-311G(d,p) calculations.

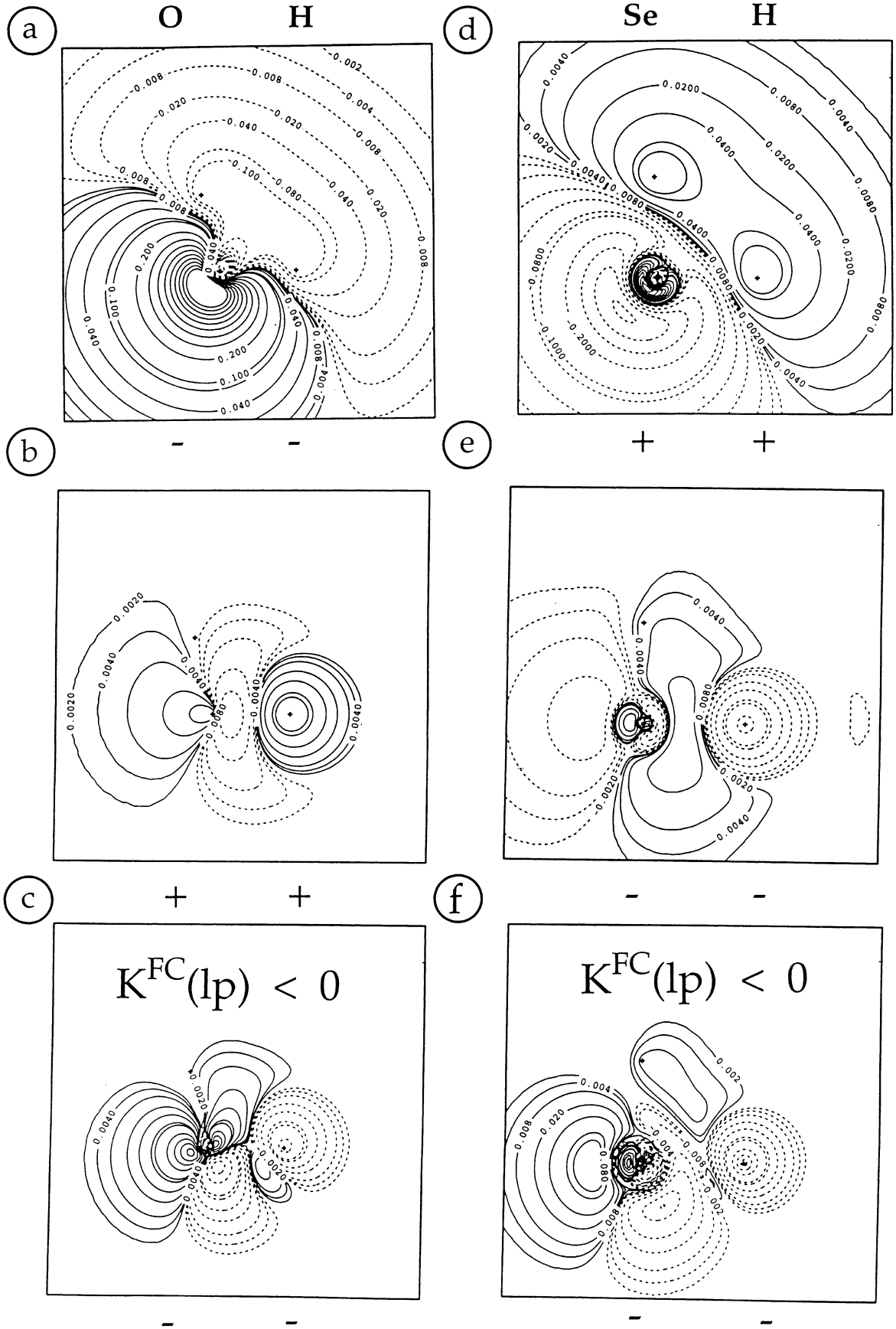

Figure 4. Contour line diagram of (a) the lone pair LMO at O of OH_2, (b) the first-order lone pair LMO at O of OH_2, (c) the FC spin density distribution of the lone pair orbital at O of OH_2, (d) the lone pair LMO at Se of SeH_2, (e) the first-order lone pair LMO at Se of SeH_2, and (f) the FC spin density distribution of the lone pair orbital at Se of SeH_2. The perturbation is always at H2. Solid contour lines indicate the positive orbital phase (spin density distribution, i.e., more α-density); dashed contour lines, the negative orbital phase (spin density distribution, i.e., more β-density). The sign of orbital and spin density at the coupling nuclei are given below each diagram. B3LYP/6-311G(d,p) calculations.

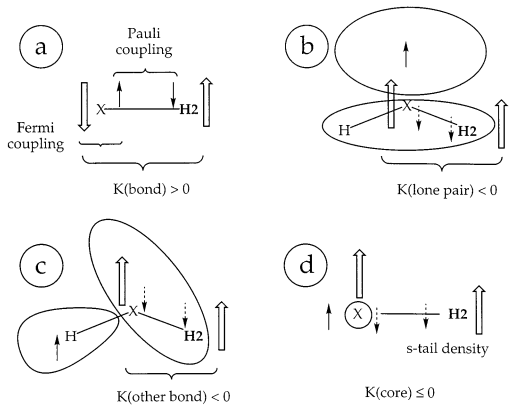

Figure 5. Extended Dirac models of the orbital contributions to the SSCC ^1K(XH). Large arrows indicate the α- and β-spin of the nucleus; small arrows, the α- and β-spin of the electron. The perturbed nucleus is the H2 in bold print, which is assumed to have always α-spin and which is the starting point of spin polarization. Solid arrows refer to specific electrons, but dashed arrows indicate the spin density distribution rather than belonging to single electrons. The diffuse back lobes of the hybrid orbitals are indicated by large ellipses. Note that only the spin density at the position of the nuclei is schematically represented, however not that in other parts of the molecule.

minor role (see Table 6) so that the influence of the electronegativity dominates. The larger the electronegativity of X is, the larger is the contraction of s-density toward the nucleus (see Table 6) and the larger becomes the spin polarization at the nucleus. An electronegative atom transmits the spin polarization caused by the magnetic moment of the nucleus and mediated by the valence bond density in a better way to the proton than a more electropositive central atoms X does.

Although the contact density is a necessary condition for a large FC term, the polarizability is a sufficient condition for the transmission of spin polarization from one nucleus to the other. The polarizability changes for second row atoms X from a large (5.4 Å^3) to a relatively small value (2.2 Å^3) for increasing atomic number, which means that the transmission of spin polarization is weakened. Hence, the minimum for the bond orbital contribution (95.4 SI units, see Table 5) of ^1K(PH) is a result of a strong decrease in the polarizability of X (from 5.38 to 3.63 Å^3) and a moderate increase of the electronegativity (from 1.90 to 2.19, Table 6). The same argument applies to the third period. They lead to a parabola behavior of the bond contribution values to ^{1}K(X,H): SiH_4, 115.8; PH_3, 95.4; H_2S, 132.1; HCl, 177.0 or GeH_4, 322.8; AsH_3, 206.3; H_2Se, 262.9; HBr, 326.1 SI units (see Table 5, second column).

Considering the bond contributions within a group, one realizes that they do not always follow the s-density calculated at the nucleus X. The s-densities of the bond orbitals have a minimum for second period atoms X (provided X has an electron lone pair) whereas the orbital contributions steadily increase within a group with increasing atomic number. The latter effect can be explained by a three- to 4-fold increase of the polarizability of X accompanied by a moderate decrease (by a factor 1.2 to 1.4) of the electronegativity (Table 6).

The trend in the s-density of the bond orbital at X can be explained in the following way. The bond orbital penetrates with its tail the core region where it is contracted in the vicinity of the nucleus. The degree of contraction can be estimated by the effective atomic charge of a nucleus (calculated according to Slater rules) experienced by a valence electron occupying the bond orbital. The effective atomic number increases from the second to the third period by an amount more than twice as large as the increase from the first to the second period (for example: F, 4.15; Cl, 11.25; Br, 29.25). Hence the contraction of the bond orbital in the core region should follow this trend, thus yielding higher s-densities from period 1 to period n (n > 1). At the same time, the p-character of the bond orbital increases while its s-character decreases with increasing atomic number in a group. This is responsible for the decrease in the HXH bond angle and can be traced back to a second-order Jahn−Teller effect. The two opposing effects (orbital contraction in the core region and decrease of the s-character of the bond orbital) lead to a minimum in the s-density at the nucleus for second period atoms (relative to the s-density of the corresponding first and third period atoms in a group; Table 6).

The absolute magnitude of the lone pair contributions to the FC term follows the polarizability of the corresponding atom X, which depends on its position within a group of the periodic table; however, it follows also the electronegativity of X, which increases within a period of the periodic table. In this respect one might argue that the number of lone pairs increases from one (group V) to three (group VII). However, each additional lone pair orbital is of π-type character (density at the nucleus is zero; no Fermi contact interaction) and, accordingly, their influence on the FC term is nil. This is different for the contributions resulting from other X−H bonds. There are three for X being a group IV element, two for X being in group V, and just one for X being a group VI element. Considering this, the polarizability effect seems to be the most important for the ob contributions.

The magnitude of the bond orbital contributions is larger than that of the lone pair contributions, which in turn are larger than the ob contributions. The core contributions are the smallest (close to zero, Table 1) because the tails of these orbitals hardly reach the H nucleus. We note that other orbital decomposition schemes fail to give reasonable core contributions.[15,16] The interaction contributions follow the trends found for the one-orbital contributions. Hence, the magnitude of the (b,lp) contributions is much larger than that of the (b,ob) or (lp,ob) contributions whereas other contributions, including core orbitals, are negligible.

In conclusion, sign and relative magnitude of one- and two-orbital contributions to the FC term of ^1K(XH) can be explained. For the sign of a particular orbital contribution one has only to consider the nodal behavior of the corresponding zeroth-order LMO, which leads to the phase at the coupling nuclei, determining also the signs in the first-order orbital and by this the signs of the spin density contribution at the nuclei. The product of the calculated spin densities at the nuclei for a given LMO provides a direct measure of the magnitude of the FC orbital contribution. Electronegativity and polarizability of X help to rationalize the relative magnitude of an orbital contribution.

3.3. Magnitude and Sign of the Orbital Contributions to PSO, SD, and DSO Terms. Distinct from the FC and SD terms, the PSO and DSO terms are mediated by orbital currents rather than spin polarization. Still, there are parallels between the PSO and FC coupling mechanisms, and the PSO coupling can be discussed in terms of zeroth- and first-order orbitals in a similar way as the FC coupling.

The magnitude of the PSO orbital contributions is in general much smaller than that of the corresponding FC contributions. All orbital interaction terms are negligible for the system investigated. For the PSO term, only the portion of exact exchange used in the exchange functional leads to a coupling in the CPDFT equations and the to two-orbital contributions.[18] The B3LYP functional uses only 20% exact exchange,[22] which explains the small two-orbital terms. Among the one orbital terms

the lone pair contributions are most important followed by the other bond, bond, and core contributions. The PSO one-orbital contributions have, apart from a few exceptions, always the opposite sign than the FC one-orbital contributions. Because the positive lp contribution dominates the PSO term, the latter is sizable and positive for those XH_n molecules, which possess one or more lone pairs.

The sign of the PSO term can be explained by considering that the PSO operator (eq 6) implies that the nabla operator is applied to the first-order orbital. For a perturbation at H2 the nodal structure of all first-order orbitals is similar, as should be the nodal structure of the gradient of the first-order orbitals. The signs at X and H are the same for the first-order orbitals when X is in the first period, but opposite in the bond region (see above). The gradient of the first-order orbitals changes sign in the bond region and leads in consequence to opposite signs at the nuclei. Hence, the positive FC bond orbital contributions imply negative PSO orbital contributions and the negative FC lone pair contributions positive PSO lone pair contributions.

Whereas for the FC contribution, occupied s-orbitals lead to large contributions, occupied pπ-orbitals (or unoccupied π^* orbitals) yield large contributions in the case of the PSO term. The nucleus interacts via the dipole field of its magnetic moment with the field generated by the movement of the electrons in a pπ-orbital. This leads to the induction of orbital currents, which have for DSO and PSO terms opposite directions weakening or strengthening the magnetic field of the nucleus. The PSO interaction is large for the pπ-lone pair orbital(s) in XH_2 and XH, where again polarizability and electronegativity play an important role. This can be rationalized in orbital language by considering that the PSO operator is an angular momentum operator and that excitations lp(X) $\rightarrow$ $\sigma^*(XH)$, $\sigma(XH)$ $\rightarrow$ Rydberg-p(X), etc. play an important role. With increasing electronegativity, the virtual orbitals adopt lower energies, thus increasing the corresponding PSO orbital currents. Alternatively, one could say that the magnitude of the PSO orbital interaction increases because a contracted pπ-orbital interacts more strongly with the dipole field of the nucleus. A larger polarizability implies more diffuse occupied orbitals and a higher orbital energy and again a larger PSO orbital current induced by the nuclear spins. Within a group, electronegativity and polarizability have opposing influences so that again a minimum of the PSO orbital contributions (lp, b, or ob) is found for X being a second period atom.

There are only a few SD orbital contributions that are larger than 1 SI unit, namely, the bond orbital and lone pair orbital contributions of those XH_n molecules that possess π-type lone pair orbitals and whose bond orbitals are dominated by p-contributions. For the SD term the dipole fields of the coupling nuclei interact via the electron density; i.e., the spin dipole field of the perturbed nucleus H leads to a spin polarization of the electrons in orbital *k*, which has to readjust at the position of nucleus X to keep the antisymmetry of the wave function. Hence, the spin dipole field of nucleus X experiences the change in the spin polarization caused by the dipole field of H and mediated by the spin density of orbital *k*. Considering the form of the dipole field of a nucleus, a p- or d-orbital can much better transmit the SD effect than an s-orbital. Also, the two-orbital effects should only be large in that case, in which the coupling nuclei possess both occupied p-orbitals. For XH_n, this is not the case and therefore the interaction terms are all relatively small.

The SD bond orbital and SD lone pair orbital contributions have the same signs as the corresponding PSO contributions; i.e., bd and lp contributions have opposite signs. Because they are of similar magnitude, they cancel each other out to a large extent, thus leading to relatively small total SD contributions. There is again a minimum in the orbital contributions for X being an element of the second period, which indicates the influence of two opposing effects, namely, electronegativity and polarizability of atom X on the SD bond orbital and SD lone pair orbital contributions.

SCHEME 2: Signs of the Orbital Contributions to the DSO Term of the SSCC[a]

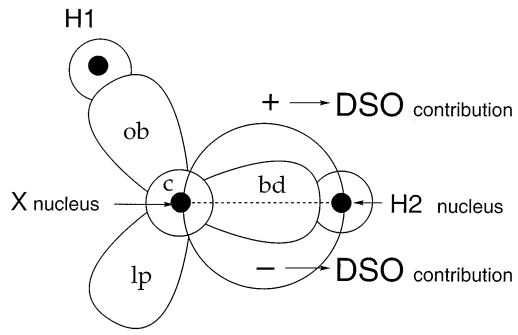

[a] Electron density inside the sphere around the X1H2 bond leads to a negative contribution; electron density outside this sphere leads to a positive contribution to the DSO term.

Due to the large number of individual contributions and the more complicated structure of the first-order KS operator, the sign and magnitude of the SD terms cannot be discussed as easily as those for the FC terms. One can, however, make plausible that SD and FC terms have opposite signs: The nuclear magnetic field for the SD term is partly opposite to that of the FC term. Hence, the SD contribution should partly compensate the FC contribution. It is noteworthy that this partial compensation takes place for each orbital separately, not only in the sum.

DSO orbital contributions are all negligible (Table 4) although some of the bd and lp contributions are in the range of 1 SI unit. Because the DSO term depends just on the zeroth-order density, it can only be large in those cases in which, due to a strong electronegativity of X, the density is contracted. Accordingly, the DSO orbital contribution should increase in magnitude from left to right in a period and from bottom to top in a group, thus yielding the largest values for FH (Table 4). But even then the orbital contribution is relatively small in view of the small zeroth-order density at the H nucleus (Table 6). Again, bd and lp LMO contributions have opposite signs (Table 4). Because they are also of comparable magnitude, they largely cancel each other so that the total DSO orbital contributions are all close to zero.

As has been shown in ref 18, a spherical charge distribution around one of the two coupling nuclei makes only a little contribution to the DSO part of the SSCC. This explains immediately that the c contributions to the DSO terms are negligible (see Scheme 2). The bd, ob, and lp charges are distinctly nonspherical around X. However, their sum is approximately spherical around X, and the parts of the bd and ob densities located at the H atoms are s-dominated and thus spherical as well. This explains that the lp and bd contributions nearly cancel each other. Generally, those parts of the charge distribution that are inside the sphere around the axis X−H2 make negative contributions to the DSO terms, and charges outside this sphere make positive contributions.[18] As shown in Scheme 2, this implies that the bd contributions are negative, whereas the lp and ob contributions are positive (the nonspherical part of the ob contributions is outside the sphere).

3.4. Trends in the Total NMR Spin−Spin Coupling Constant. The largest contributions to ^1K(XH) result from the FC term and the PSO term whereas the total SD and DSO orbital contributions can be neglected in a discussion of the trends in the calculated ^1K(XH) values. For XH_n molecules without lone pair electrons (X from group IV) the SSCC ^1K(XH) is clearly dominated by the FC term, which in turn is dominated by the bond orbital contribution (CH_4 total 39.2, FC 38.5, FC(bd) 52.1; SiH_4 total 78.2, FC 78.3, FC(bd) 116.1; GeH_4 total 193.8, FC 194.3, FC(bd) 322.7 SI units; see Tables 1 and 5). The dependence of the bd orbital contribution on electronegativity and polarizability is equally valid for the dependence of the total SSCC ^1K(XH). The negative ob and (b,ob) contributions lead to the actual value of ^1K(XH).

The lp contributions change the trend in the calculated SSCCs. The latter no longer increase within a group but they decrease. For the XH_3 molecules, the influence of the (positive) PSO orbital contributions is moderate. Decisive are the negative FC(lp) and FC(bd,lp) contributions, which revert the trend in the positive FC(bd) orbital contributions so that a decrease of the SSCC ^1K(XH) with increasing atomic number in a group results.

For the XH_2 molecules, which possess a π-type and a σ-type lone pair the influence of the positive PSO orbital contribution becomes decisive. It does not change the trend determined by the FC orbital contributions, but it changes the negative SSCC $^1K^{FC}$(SeH) into a positive SSCC ^1K(SeH).

For the XH molecules, the PSO term becomes more important than the FC term for FH and ClH whereas for BrH the (negative) FC term is more important, leading to a negative value of ^1K(BrH). One might criticize this interpretation because of the large deviation of calculated from measured ^1K(XH) values (see Table 5). Therefore, we have repeated SSCC calculations with Dunning's cc-pVQZ basis set. In this way, the deviation between calculated and measured SSCCs could be reduced by 50% (Table 5). Still some of the calculated ^1K(XH) values differ by 12−20 SI units (Table 5). Four different effects can be responsible for these deviations. (a) It is well-known that basis sets for which the inner shell parts are augmented by additional s-functions or, alternatively, decontracted are better suited for obtaining high-accuracy values of SSCCs.[31] (b) DFT may include important dynamic and nondynamic correlation needed for the calculation of SSCCs. However, this does not imply that all electron correlation effects are included that guarantee a reliable description of SSCCs. (c) In a recent investigation of NMR chemical shieldings, Filatov and Cremer[32] have shown that the relativistic changes in both diamagnetic and paramagnetic contributions are substantial. The former are caused by a relativistic contraction of s- and p-orbitals of the heavy atoms and the latter are due to a secondary effect, namely, the expansion of d- and f-orbitals. The contraction of the s-orbitals will lead to substantially larger SSCC ^1K(XH) values and explains why nonrelativistic calculations underestimate the SSCCs. In the case of the XH_n molecules with lone pair electrons, the PSO term will have substantial relativistic changes where, however, trends are difficult to foresee. (d) Finally, we have to emphasize that measured SSCCs represent vibrational averages, which differ considerably from SSCCs calculated for the equilibrium geometry. Calculations show that differences as large as 5% can be observed for ^{1}J(XH) SSCCs.[33]

4. Conclusions

Trends in calculated and measured one-bond SSCC ^1K(XH) values for twelve XH_n hydrides (X = C, Si, Ge, N, P, As, O, S, Se, F, Cl, Br) have been explained using orbital contributions obtained with the J-**OC**-PSP approach. The sign and magnitudes of the orbital contributions have been rationalized with the help of the Fermi contact spin density distribution, the s-density of an orbital at the nucleus, the electronegativity, and the polarizability of the central atom X.

(1) The one-bond SSCC ^1K(XH) is influenced in sign and magnitude by several one-orbital and two-orbital contributions, which behave differently with atomic number *Z*. Therefore, it is almost impossible to rationalize trends in measured one-bond SSCC ^1K(XH) values of XH_n hydrides by one simple concept, as has been repeatedly tried in the literature.

(2) The assumption that the FC term leads to the most important contribution to the SSCC ^1K(XH), which is often found in the literature, cannot be confirmed. The PSO term becomes equally important in the case of heteroatoms X with electron lone pairs. The DSO and SD terms are only small because bond and lone pair contributions have opposite signs and lead to a large cancellation of these contributions.

(3) With the help of the Fermi contact spin density distribution, the sign of the FC orbital contributions can be predicted for the one-orbital terms. In the case of the two-orbital terms, sign predictions are also possible but require that the relative magnitude of the terms ($x \leftarrow y$) and ($y \leftarrow x$) contributing to (x,y) can be estimated when they possess different signs. Sign predictions are possible in the case of SSCC ^1K(XH) because of the regular nodal structure of zeroth- and first-order LMO. All first-order LMOs are dominated by the antibonding X−H2 LMO (provided H2 is perturbed) and therefore have always the same nodal structure. The same sign relationships are found for the dominant orbital contribution irrespective of the period and the group atom X is located in.

(4) The magnitude of the FC term of ^1K(XH) is strongly influenced by a positive bond LMO contribution, which increases within a group and the first period but shows a parabola behavior within the second and third period. It is demonstrated that an efficient spin coupling mechanism requires both a large electronegativity (leading to a large contact spin density at the nucleus) and a large polarizability of X (leading to an effective transmission of spin polarization). The increase of the bond orbital term within a group results from an increase in the polarizability, and that within a period from an increased electronegativity. In period 2 and 3 the two effects are counteractive, thus leading to a parabola behavior of the bond orbital contributions to the FC term.

(5) The lone pair and (bd,lp) contributions to the spin-coupling mechanism are the most important for the FC term. They are both negative, which can be explained by inspection of the FC spin density distribution (see Figure 5). The negative (bd,lp) two-orbital contribution is the sum of a large negative lp ← bd and a smaller positive bd ← lp contribution. Again the calculated trends in the lp terms can be explained by the increasing polarizability of X within a group and the increasing electronegativity of X within a period.

(6) The PSO term will be only large if X is a heteroatom because only the π-type lone pair orbitals are significantly involved in the PSO spin−spin coupling mechanism. The sign of the lp one-orbital contribution is always positive, as can be predicted considering the gradient of the first-order orbitals. Again, increasing polarizability and increasing electronegativity of X determine the magnitude of the PSO lp-term where, however, also an increasing number of occupied π-type lone pair orbitals plays an important role.

(7) Analysis of the SD orbital contributions to the spin−spin coupling mechanism can be simplified by realizing that the

nuclear magnetic field for the SD term is partly opposite to that of the FC term. Accordingly, the SD orbital contributions have a sign opposite to that of the corresponding FC orbital contributions, thus partly compensating the FC term. Considering the form of the dipole field of a nucleus, an occupied p- or d-orbital can much better transmit the SD effect than an occupied s-orbital. The bd and lp contributions have opposite signs. Because they are of similar magnitude, they cancel each other out to a large extent, thus leading to relatively small total SD contributions.

(8) The DSO contributions just depend on the zeroth-order electron density, which increases at the nucleus with increasing electronegativity. A spherical charge distribution around one of the two coupling nuclei makes only a little contribution to the DSO part of the SSCC. The bd, ob, and lp charge distributions around the nucleus X are nonspherical. However, their sum is approximately spherical around X so that the lp and bd contributions nearly cancel each other. Generally, those parts of the density distribution that are inside (outside) a sphere around the axis X−H2 lead to negative (positive) contributions to the DSO terms, thus explaining why the bd contributions are negative, whereas the lp and ob contributions are positive (see Scheme 2).

(9) The largest contributions to ^1K(XH) result from the FC term and the PSO term whereas the total SD and DSO orbital contributions can be neglected. For XH_n molecules without lone pair electrons (X from group IV) the SSCCs ^1K(XH) is clearly dominated by the FC term, which in turn is dominated by the bond orbital contribution. The lp contributions change the trend in the calculated SSCCs. The latter no longer increase within a group, but they decrease. For the XH_3 molecules, the negative FC lp and FC (b,lp) contributions are decisive because they reverse the trend in the positive FC bd orbital contributions so that a decrease of the SSCC ^1K(XH) with increasing atomic number in a group results. For the XH_2 molecules, the positive PSO orbital contribution becomes decisive. It does not change the trend determined by the FC orbital contributions, but it changes the negative SSCC $^1K^{FC}$(SeH) into a positive SSCC ^1K(SeH). For the XH molecules, the PSO term becomes more important than the FC term for FH and ClH whereas for BrH the (negative) FC term is more important, leading to a negative value of ^1K(BrH).

(10) Calculated SSCC ^1K(XH) values are improved by using Dunning's cc-pVQZ basis set. The remaining differences between calculated and measured values can be due to (a) additional basis set inefficiencies, (b) lack of higher order correlation effects, (c) relativistic effects, or (d) vibrational effects.

Acknowledgment. This work was supported by the Swedish Research Council (Vetenskapsrådet). Calculations were done on the supercomputers of the Nationellt Superdatorcentrum (NSC), Linköping, Sweden. D.C. thanks the NSC for a generous allotment of computer time.

References and Notes

(1) See, e.g.: *Encyclopedia of Nuclear Magnetic Resonance*; Grant, D. M., Harris, R. K., Eds.; Wiley: Chichester, UK, 1996; Vols. 1−8.

(2) Webb, G. A., Ed. *Specialist Periodical Reports, Nuclear Magnetic Resonance*; Chapters on applications of spin−spin couplings; The Royal Society of Chemistry, 1983−1992; Vols. 12−28.

(3) (a) Kowalewski, J. *Prog. NMR Spectrosc.* **1977**, *11*, 1. (b) Kowalewski, J. *Annu. Rep. NMR Spectrosc.* **1982**, *12*, 81.

(4) Contreras, R. H.; Facelli, J. C. *Annu. Rep. NMR Spectrosc.* **1993**, *27*, 255.

(5) Contreras, R. H.; Peralta, J. E. *Prog. NMR Spectrosc.* **2000**, *37*, 321.

(6) Marshall, J. L. *Carbon−carbon and carbon-proton NMR couplings: Applications to Organic Stereochemistry and Conformational Analysis*; Verlag Chemie Int: Deerfield Beach, FL, 1983.

(7) Marchand, A. P. *Stereochemical Application of NMR studies in Rigid Bicyclic Systems*; VCH: Deerfield Beach, FL, 1982.

(8) (a) Tvaroska, I.; Taravel, F. R. *Adv. Carbonhydr. Chem. Biochem.* **1995**, *51*, 15. (b) True, N. S.; Suarez, C. *Adv. Mol. Struct. Res.* **1995**, *1*, 115. (c) Thomas, W. A. *Prog. NMR. Spectrosc.* **1997**, *30*, 183.

(9) (a) Karplus, M.; Anderson, D. H. *J. Chem. Phys.* **1959**, *30*, 6. (b) Karplus, M. *J. Chem. Phys.* **1959**, *30*, 11. (c) Karplus, M. *J. Am. Chem. Soc.* **1963**, *85*, 2870.

(10) For a recent review, see: Altona, C. In *Encyclopedia of Nuclear Magnetic Resonance*; Grant, D. M., Harris, R. K., Eds.; Wiley: Chichester, U.K., 1996; p 4909.

(11) (a) Wu, A.; Cremer, D.; Auer, A. A.; Gauss, J. *J. Phys. Chem. A* **2002**, *106*, 657. (b) Wu, A.; Cremer, D. *Int. J. Mol. Sci.* **2003**, *4*, 159. (c) Wu, A.; Cremer, D. *J. Phys. Chem. A* **2003**, *107*, 1797. (d) Sychrovsky, V.; Vacek, J.; Hobza, P.; Zidek, L.; Sklenar, V.; Cremer, D. *J. Phys. Chem. B* **2002**, *106*, 10242.

(12) (a) Barfield, M. Indirect Coupling: Theory and Applications in Organic Chemistry. *Encyclopedia of NMR*; Wiley: New York, 1996; p 2520. (b) Barfield, M.; Chakrabarty, B. *Chem. Rev.* **1969**, *69*, 757.

(13) (a) Engelmann, A. R.; Contreras, R. H.; Facelli, J. C. *Theo. Chim. Acta* **1981**, *59*, 17. (b) Engelmann, A. R.; Contreras, R. H. *Int. J. Quantum Chem.* **1983**, *23*, 1033. (c) Scuseria, G. E.; Facelli, J. C.; Contreras, R. H.; Engelmann, A. R. *Chem. Phys. Lett.* **1983**, *96* 560. (d) Contreras, R. H.; Scuseria, G. E. *Org. Magn. Reson.* **1984**, *22*, 411. (e) Diaz, A. C.; Giribet, C. G.; Ruiz De Azua, C. C.; Contreras, R. H. *Int. J. Quantum Chem.* **1990**, *37*, 663. (f) Aucar, G. A.; Zunino, V.; Ferraro, M. B.; Giribet, C. G.; Ruiz de Azua, M. C.; Contreras, R. H. *J. Mol. Struct. (THEOCHEM.)* **1990**, *205*, 63. (g) Aucar, G. A.; Ruiz de Azua, M. C.; Giribet, C. G.; Contreras, R. H. *J. Mol. Struct. (THEOCHEM.)* **1990**, *205*, 79.

(14) Contreras, R. H.; Peralta, J. E.; Biribet, C. G.; Ruiz De Azua, M. C.; Faceli, J. C. *Annu. Rep. NMR. Spectrosc.* **2000**, *41*, 55.

(15) (a) Peralta, J. E.; Contreras, R. H.; Snyder, J. P. *Chem. Commun.* **2000**, 2025. (b) Barone, V.; Provasi, P. F.; Peralta, J. E.; Snyder, J. P.; Sauer, S. P. A.; Contreras, R. H. *J. Phys. Chem. A*, in press.

(16) Wikens, S. J.; Westler, W. M.; Markley, J. L.; Weinhold, F. *J. Am. Chem. Soc.* **2001**, *123*, 12026.

(17) Ramsey, N. F. *Phys. Rev.* **1953**, *91*, 303.

(18) Sychrovsky, V.; Gräfenstein, J.; Cremer, D. *J. Chem. Phys.* **2000**, *113*, 3530.

(19) Helgaker, T.; Watson, M.; Handy, N. C. *J. Chem. Phys.* **2000**, *113*, 9402.

(20) Wu, A.; Cremer, D. *J. Am. Chem. Soc.*, submitted for publication.

(21) For a summary of experimental SSCCs of XH_n molecules, see ref 3b.

(22) Becke, A. D. *J. Chem. Phys.* **1993**, *98*, 5648.

(23) Becke, A. D. *Phys. Rev. A* **1988**, *38*, 3098.

(24) Lee, C.; Yang, W.; Parr, R. P. *Phys. Rev. B* **1988**, *37*, 785.

(25) (a) Frisch, M. J.; Pople, J. A.; Binkley, J. S. *J. Chem. Phys.* **1984**, *80*, 3265. (b) Hariharan, P. C.; Pople, J. A. *Theor. Chim. Acta* **1973**, *28*, 213.

(26) Dunning, T. H., Jr. *J. Chem. Phys.* **1989**, *99*, 107.

(27) Boys, S. F. *Rev. Mod. Phys.* **1960**, *32*, 296.

(28) Kraka. E.; Gräfenstein; J.; Filatov, M.; He, Y.; Gauss, J.; Wu, A.; Polo, V.; Olsson, L.; Konkoli, Z.; He. Z.; Cremer D. COLOGNE2003, Göteborg University, Göteborg, 2003.

(29) Frisch, M. J.; Trucks, G. W.; Schlegel, H. B.; Scuseria, G. E.; Robb, M. A.; Cheeseman, J. R.; Zakrzewski, V. G.; Montgomery, J. A., Jr.; Stratmann, R. E.; Burant, J. C.; Dapprich, S.; Millam, J. M.; Daniels, A. D.; Kudin, K. N.; Strain, M. C.; Farkas, O.; Tomasi, J.; Barone, V.; Cossi, M.; Cammi, R.; Mennucci, B.; Pomelli, C.; Adamo, C.; Clifford, S.; Ochterski, J.; Petersson, G. A.; Ayala, P. Y.; Cui, Q.; Morokuma, K.; Malick, D. K.; Rabuck, A. D.; Raghavachari, K.; Foresman, J. B.; Cioslowski, J.; Ortiz, J. V.; Stefanov, B. B.; Liu, G.; Liashenko, A.; Piskorz, P.; Komaromi, I.; Gomperts, R.; Martin, R. L.; Fox, D. J.; Keith, T.; Al-Laham, M. A.; Peng, C. Y.; Nanayakkara, A.; Gonzalez, C.; Challacombe, M.; Gill, P. M. W.; Johnson, B. G.; Chen, W.; Wong, M. W.; Andres, J. L.; Head-Gordon, M.; Replogle, E. S.; Pople, J. A. *Gaussian98*, revision A.5; Gaussian, Inc.: Pittsburgh, PA, 1998.

(30) *CRC Handbook of Chemistry and Physics on CD-ROM*, 2000 Version. Lide, D. R., Ed.; CRC Press LLC: Boca Raton, FL, 2000.

(31) Helgaker, T.; Jaszunski, M.; Ruud, K.; Gorska, A. *Theor. Chem. Acc.* **1998**, *99*, 175. (b) Enevoldsen, T.; Oddershede, J.; Sauer, S. P. A. *Theor. Chem. Acc.* **1998**, *100*, 275.

(32) Filatov, M.; Cremer, D. *J. Chem. Phys.* **2003**, *119*, 701.

(33) Ruden, A. T.; Lutnas, O. B.; Helgaker, T.; Ruud, K. *J. Chem. Phys.* **2003** *118*, 9572 and references therein.